Inorganic Chemistry Communications 138 (2022) 109308

Contents lists available at ScienceDirect

Inorganic Chemistry Communications

journal homepage: www.elsevier.com/locate/inoche

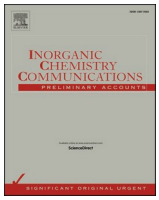

Short communication

Elaboration, characterization and applications of SnO_2, 2 %Gd-SnO_2 and 2 %Gd-9 %F-SnO_2 thin films for the photocatalytic degradation of MB by USP method

Sabrina Roguai *, Abdelkader Djelloul

LASPI²A Laboratoire des Structures, Propriétés et Interactions Inter Atomiques, Université Abbes Laghrour, Khenchela 40000, Algeria
Department of Science of matter, Abbes Laghrour University, Khenchela, Algeria

ARTICLE INFO

Keywords:
SnO_2
2%Gd-SnO_2
and 2%Gd-9%F-SnO_2 films
X-ray diffraction
SEM
EDAX
FTIR
and Optical properties
Electrical properties
Photocatalytic

ABSTRACT

In this study, SnO_2, 2 %Gd-SnO_2, and 2 %Gd-9 %F-SnO_2 films were grown from tin chloride solutions by the ultrasonic spray technique on ordinary microscope glass substrates heated to a fixed temperature of 450 °C for photocatalytic application. The microstructural characterization of the thin films obtained was performed using X-ray diffraction (XRD), SEM, EDAX, and Infrared Spectroscopy (IR). The optical properties of thin films were studied by UV–Visible spectroscopy. To examine the electrical properties, we use the four-point method, the Seebeck effect and the Mott Shottky analysis. X-ray difraction reveals the formation of the routile phase of SnO_2 in all thin films with average crystallite size estimated in the range of 24–62 nm. The co-doping in (Gd-F) permitted an improvement of the thermoelectric properties of SnO_2. Moreover, we have demonstrated that an increase in grain size allows toimprove the Seebeck coefficient, to increase the electrical conductivity, on the other hand the doping in (Gd), presents a decrease in the size of the crystallites, which improves the degradation of methyl blue. The UV–Visible spectra of optical transmission of the layers show that the pure, doped and co-doped SnO2 films are of good quality with a transmittance of 73–83% in the visible and have an optical gap evaluated between 3.89, 3.98 and 3.99 eV respectively.

1. Introduction

The tin oxide is an n-type semiconductor with a broad bandwidth ranging from 2.7 to 4.6 eV, with a full valence band derived from the O 2p level (O^{2-} :$1s^2$ 2 s^2 $2p^6$ 3 s^0) and an empty conduction band from the Sn 5 s level [1]. The electronic configuration of tin (Sn: 1 s2 2 s2 2p6 3 s^2 $3p^6$ 4 s2 $3d^{10}$ $4p^6$ $4d^{10}$ 5 s^2 $5p^2$) provides for two sets of organic combinations corresponding to valences 4 and 2, tin finds the much more stable valence 4. The p states of oxygen represent a band at bond energies between 0 and 2 eV, this constitutes an energy band of 2 to 5 eV between the Sn 5p and O 2p orbitals. The lowest part of the valence band would result from strong interactions between the Sn 5 s and O 2p states. The last core levels of Sn 4d tin (the Sn 4d5/2 and Sn 4d3/2 states) are located at 22.2 and 23.2 eV respectively. The valence band is characterized by a high binding energy with hybridization of O 2p-Sn 5 s and O 2p-Sn 5p [1]. Regarding the conduction band, the lowest empty energy level is Sn 5 s, followed by Sn 5p states [1]. The interest of compounds with a band gap energy higher than 3.6 eV lies in the transparency in visible light of these compounds. On the other hand, this band gap energy is large enough not to allow carrier activation at high temperature, a process that strongly decreases the Seebeck coefficient. SnO_2 presents a single stable phase at atmospheric pressure, known as cassiterite and adopts a quadratic rutile type lattice.

Tin oxide crystallizes with a rutile-type tetragonal structure [2-4]. Its lattice (a = b = 4.737 Å and c = 3.185 Å) contains six atoms [5]: two tin atoms (RSn^{4+}= 0.71 Å) and four oxygen atoms (RO^{2-}=1.40 Å). Each tin atom is the center of an almost regular octahedron formed by six oxygen atoms, while each oxygen atom is surrounded by three tin atoms located at the vertices of an isosceles triangle. The description of the crystallographic orientation of the lattice varies according to the method of elaboration of the tin oxide [6]. Oxygen vacancies in thin films are the predominant type of defect, and interstitial tin atoms can easily diffuse to the surface and be oxidized there. COX et al [7] classify these vacancies into bulk and surface vacancies. Oxygen vacancies in the tin oxide layers result in an n-type semiconductor [6]. The concentration of electrons in pure SnO_2 results primarily from a lack of stoichiometry [8],

* Corresponding author.
E-mail address: rog.sabrina@yahoo.fr (S. Roguai).

https://doi.org/10.1016/j.inoche.2022.109308
Received 6 December 2021; Received in revised form 10 February 2022; Accepted 13 February 2022
Available online 17 February 2022

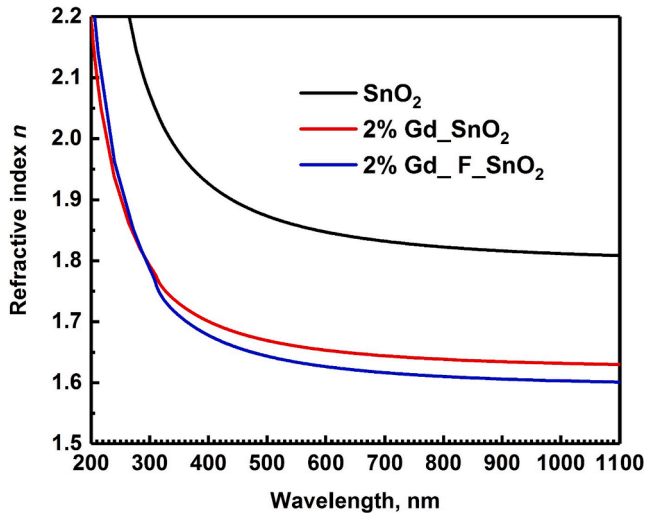

Fig. 6. Refractive index of SnO_2, 2 %Gd-SnO_2, and 2 %Gd-9 %F-SnO_2 films.

Table 4
Surface resistance, resistivity and electrical conductivity of SnO_2, 2 %Gd-SnO_2 and 2 %Gd-9 %F-SnO_2 thin films

Samples	Square resistance, Ω	resistivity (×10^{-2}), Ω cm	Conductivity, Ω^{-1} cm^{-1}
SnO_2	260	1.8	55
2 %Gd-SnO_2	670	2.9	10
2 %Gd-9 %F-SnO_2	380	1.3	74

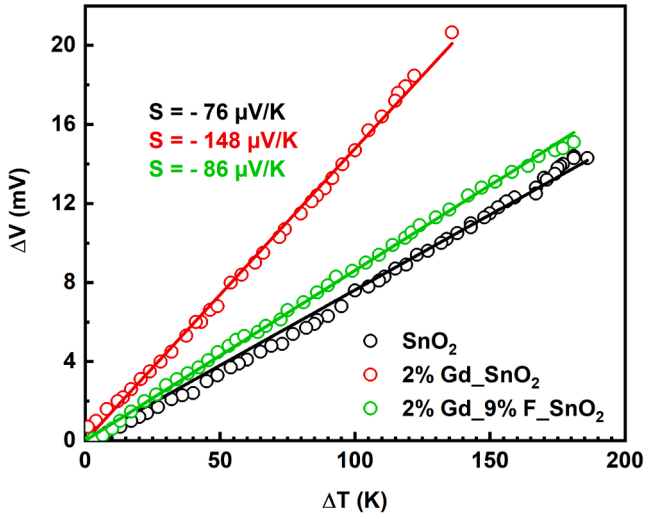

Fig. 7. Seebeck coefficients for SnO_2, 2 %Gd-SnO_2, and 2 %Gd-9 %F-SnO_2 thin films.

Table 5
Carrier concentrations (n), and Fermi energy (EF), of SnO_2, 2 %Gd-SnO_2, 2 %Gd-9 %F- SnO_2 sprayed thin films.

	n, cm^{-3}	E_F, meV
SnO_2	1.9×10^{19}	96
2 %Gd _SnO_2	5.3×10^{18}	49
2 %Gd _9%F_SnO_2	1.5×10^{19}	85

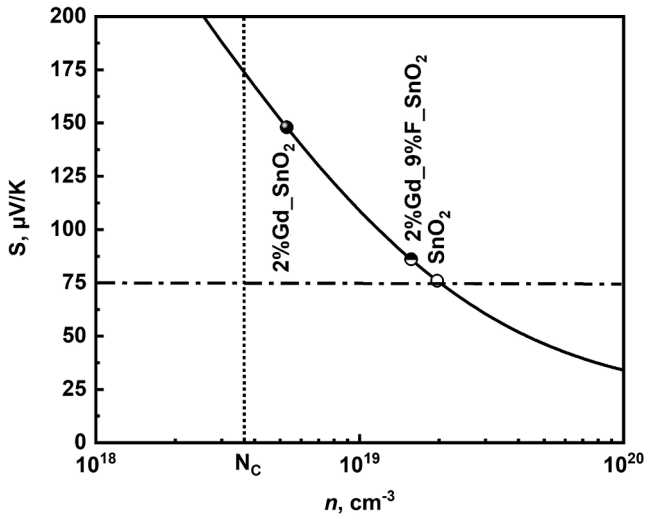

Fig. 8. Seebeck coefficients as a function of carrier concentrations for SnO_2, 2 %Gd-SnO_2, and 2 %Gd-9 %F-SnO_2 thin films.

(10), presented by the notation of KrÖger-Vink notation [63].

$$O_O^X \rightarrow V_O^{\cdot\cdot} + 2e^- + \frac{1}{2}O_2 \tag{10}$$

Moreover, this degeneracy in our samples is verified by the evaluation of the Fermi energy level (E_F) according to this relation [64]:

$$E_F = \frac{\pi^2 k_B^2 T}{3|e||S|} \tag{11}$$

The Fermi energy values calculated are listed in Table 5, the value of Fermi energy for undoped SnO_2 (96 meV) is smaller then the valus calculaterted by first-principles calculations based on the density functional theory (427 meV) [65], that indicates that our thin film elaborated by the USP technique is conductive which confirms by the previous results of the carrier concentration. For the 2 %Gd-9 %F-SnO_2 films the values of Fermi energy are 49 and 85 meV respectively, the reduction of E_F with doping can be interpreted by the substitution of Sn^{4+} ions by Gd^{3+} ions. Subsequently, the E_F values are regained with co-doping as fluorine (donor), generates the localized levels in the gap and thus change the position of the fermi level near the conduction band [6]. This can be explained as follows: when fluorine is incorporated into the tin oxide layers, each F^- anion substitutes an O^{-2} anion in the lattice and the F^- substituted anion has more free electrons because it can play the role of the O^{-2} anion with an excess electron easily ejected into the conduction band ($O^{2-} + F \rightarrow O + F^- + e^-$), this results in an increase of free electrons responsible for the decrease of the resistivity value.

3.6.3. Mott-Schottky (MS) analysis

Mott-Schottky measurements are useful for determining the charge carrier density (N_D) and flat band potential (E_{fb}) and their variation with electrolyte pH. Fig. 9 shows the M–S curves of SnO_2, 2 %Gd-SnO_2 films obtained in electrolytes at PH = 9. These curves are obtained by plotting the variation of the differential capacitance of the space charge region as a function of the potential applied in a 0.5 M Na_2SO_4 electrolyte with a frequency of 1 kHz. by applying equation (12) [66].

$$\frac{1}{C^2} = \frac{2}{\varepsilon s \varepsilon_0 A^2 e N_D}\left(V - V_{fb} - \frac{K_B T}{e}\right) \tag{12}$$

In which C corresponds to the interfacial capacitance, εs denotes the dielectric constant of the semiconductor, ε_0 the free-space permittivity, e the electronic charge, N_D the donor density, V the applied potential, V_{fb} the flat-band potential, k_B the Boltzmann constant and T the absolute temperature. The linear part of the M–S curves has a positive slope; this